

The effect of surface topography on the nonlinear dynamics of Rossby waves

By S.I. Abarzhi, O. Desjardins, H. Pitsch

1. Motivation and objectives

Boussinesq convection in rotating systems attracts a sustained attention of the fluid dynamics community, because it has intricate non-linear dynamics (Cross & Hohenberg 1993) and plays an important role in geophysical and astrophysical applications, such as the motion of the liquid outer core of Earth, the Red Spot in Jupiter, the giant cells in the Sun etc. (Alridge *et al.* 1990). A fundamental distinction between the real geo- and astrophysical problems and the idealized laboratory studies is that natural systems are inhomogeneous (Alridge *et al.* 1990). Heterogeneities modulate the flow and influence significantly the dynamics of convective patterns (Alridge *et al.* 1990; Hide 1971). The effect of modulations on pattern formation and transition to turbulence in Boussinesq convection is far from being completely understood (Cross & Hohenberg 1993; Aranson & Kramer 2002).

It is generally accepted that in the liquid outer core of the Earth the transport of the angular momentum and internal heat occurs via thermal Rossby waves (Zhang *et al.* 2001; Kuang & Bloxham 1999). These waves been visualized in laboratory experiments in rotating liquid-filled spheres and concentric spherical shells (Zhang *et al.* 2001; Kuang & Bloxham 1999). The basic dynamical features of Rossby waves have been reproduced in a cylindrical annulus, a system much simpler than the spherical ones (Busse & Or 1986; Or & Busse 1987). For convection in a cylindrical annulus, the fluid motion is two-dimensional, and gravity is replaced by a centrifugal force, (Busse & Or 1986; Or & Busse 1987). Hide (1971) has suggested that the momentum and heat transport in the core might be influenced significantly by so-called bumps, which are heterogeneities on the mantle-core boundary. To model the effect of surface topography on the transport of momentum and energy in the liquid outer core of the Earth, Bell & Soward (1996), Herrmann & Busse (1998) and Westerburg & Busse (2001) have studied the nonlinear dynamics of thermal Rossby waves in a cylindrical annulus with azimuthally modulated height.

The models of Bell & Soward (1996), Herrmann & Busse (1998), and Westerburg & Busse (2001) considered different regimes of the flow, and reported analytical and numerical solutions for the system of conservation laws. Bell & Soward (1996) assumed periodic boundary conditions in the radial direction and neglected the viscous friction in the fluid interior. They found two types of convective patterns depending on the modulation amplitude: Rossby waves for small modulation amplitude and traveling waves with long azimuthal length scale for large modulation amplitude. Herrmann & Busse (1998) and Westerburg & Busse (2001) have accounted for the viscous friction in the fluid interior, neglected the friction produced by the Eckman layer, assumed no-slip boundary conditions in the radial direction, and found Rossby waves with quasi-periodic dependencies in space and in time. Both rigorous studies, the work by Bell & Soward (1996), and by Herrmann & Busse (1998) and Westerburg & Busse (2001) compliment each other and

identify several important features of the modulated convection. A need still remains for a model, which quantitatively and qualitatively describes the effect of modulations on Rossby waves in a wide range of the forcing parameters and convection intensity, and which can compare this inhomogeneous system to other pattern-forming systems (Cross & Hohenberg 1993; Aranson & Kramer 2002). Here we suggest a model to study the effect of surface topography on the nonlinear dynamics of thermal Rossby waves.

2. Pattern-forming system with modulated forcing

For rotating cylindrical annulus with homogeneous boundary conditions, the nonlinear dynamics of thermal Rossby waves are described by a complex Ginzburg-Landau equation in terms of amplitude A , whose magnitude determines the convection intensity, and whose phase describes changes in the position and direction of the convective rolls. We refer the reader to Busse & Or (1986) and Or & Busse (1987) for details. For heterogeneous systems, a rigorous derivation of the amplitude equation from the conservation laws has not been accomplished yet (Cross & Hohenberg 1993; Aranson & Kramer 2002). To model the nonlinear dynamics of slightly inhomogeneous systems, one usually applies the Ginzburg-Landau equation with forcing. As an example, one may consider pattern formation in the presence of a mode associated with a conserved physical quantity, such as the Rayleigh-Benard convection driven by surface tension, which has been considered by Siggia & Zippelius (1981), Tribelsky & Velarde (1996), Matthews & Cox (2000). Other examples are convection in liquid crystals driven by a stochastic electric field (Meyer *et al.* 1987; Wu & Andereck 1990; Roder *et al.* 1997), and the study of the effect of time-periodic forcing on an oscillatory system (Elphick *et al.* 1987; Coulet *et al.* 1990; Hemming & Kapral 2000).

Convection in a rotating cylindrical annulus with inhomogeneous boundaries differs from the foregoing pattern-forming systems. The surface modulation is not a slowly relaxing Goldstone mode as in the models with a conserved physical quantity (Siggia & Zippelius 1981; Tribelsky & Velarde 1996; Matthews & Cox 2000). The modulation does not result in an Ising-Bloch bifurcation as in the model with time-periodic forcing (Elphick *et al.* 1987; Coulet *et al.* 1990; Hemming & Kapral 2000), and its amplitude does not change with time, in contrast to the system with stochastic forcing (Meyer *et al.* 1987; Wu & Andereck 1990; Roder *et al.* 1997). To study the effect of surface topography on the dynamics of thermal Rossby waves, the Ginzburg-Landau equation with spatially periodic and time-independent forcing is a proper model. The equation has the form:

$$\frac{\partial A}{\partial T} = \beta \frac{\partial^2 A}{\partial Y^2} + \Delta_0 A + D|A|^2 A + (\delta e^{ikY} + \delta^* e^{-ikY}) A. \quad (2.1)$$

Here T and Y are the slow time and coordinate, A is the complex amplitude, the values of β and D are complex numbers with $\beta = \beta_r + i\beta_i$, $D = D_r + iD_i$, the subscripts r and i mark the real and imaginary parts, $\Delta_0 \sim (R - R_{cr})$ is real with R_{cr} being the critical Raleigh number (Cross & Hohenberg 1993; Busse & Or 1986; Or & Busse 1987; Aranson & Kramer 2002). The forcing amplitude and the absolute value of the wave-vector are δ and k respectively, where the asterisk marks the complex conjugate. The system (2.1) is slightly inhomogeneous and $|\delta|k \ll 1$.

Without forcing, $\delta = 0$, the values of β , D , Δ_0 in the equation (2.1) can be derived from the incompressible Navier-Stokes and energy equations for $R \sim R_{cr}$ (Busse & Or

1986; Or & Busse 1987). In agreement with the stability criterion the real parts of β and D obey the relations $\beta_r > 0$ and $D_r < 0$ (Cross & Hohenberg 1993; Aranson & Kramer 2002). The dynamics of the convective rolls are described by the traveling waves with $A = \bar{A} = A_0 e^{iqy + i\gamma T}$, where

$$A_0^2 = -\frac{(\Delta_0 - \beta_r q^2)}{D_r}, \quad \gamma = -\beta_i q^2 + D_i A_s. \quad (2.2)$$

This solution appears for $\Delta_0 > \beta_r q^2$, and depicts the pattern formation of thermal Rossby waves without forcing.

If the value of Δ_0 is finite and the modulation amplitude is small, $|\delta| \ll |\Delta_0|$, the explicit dependence on the Y coordinate in equation (2.1) can be eliminated. We present the amplitude A in (2.1) in the form $A = \bar{A} + \hat{A}$, where $\bar{A} = A_0 e^{iqy + i\gamma T}$ from (2.2), and the term $\hat{A} = A_1 + A_2 + \dots$ appears due to the forcing with $A_n = (a_n e^{-inkY} + b_n e^{inkY}) e^{iqY + i\gamma T}$, $n = 1, 2, \dots$. In this way we obtain

$$A = e^{iqY + i\gamma T} [A_0 + a_1 e^{-ikY} + b_1 e^{ikY} + a_2 e^{-2ikY} + b_2 e^{2ikY} + \dots]. \quad (2.3)$$

Substituting the expression (2.3) in (2.1) and expanding the equation (2.1) in terms of small $|\delta/\Delta_0|$, we can derive a system of the coupled equations of the Ginzburg-Landau type:

$$\frac{\partial A_0}{\partial T} = [f_0 + DA_0^2 + 2D(a_1 a_1^* + b_1 b_1^* + a_1 b_1)] A_0 + a_1 \delta^* + b_1 \delta, \quad (2.4)$$

$$\frac{\partial a_1}{\partial T} = f_1^- a_1 + db_1^* + [D(a_1 a_1^* + 2b_1 b_1^*) a_1 + 2DA_0(a_1^* a_2 + a_2 b_1 + b_1 b_2^*)] + A_0 \delta + a_2 \delta^* \quad (2.5)$$

$$\frac{\partial b_1}{\partial T} = da_1^* + f_1^+ b_1 + [D(2a_1 a_1^* + b_1 b_1^*) b_1 + 2DA_0(a_1 a_2^* + a_1 b_2 + b_1^* b_2)] + A_0 \delta^* + b_2 \delta, \quad (2.6)$$

$$\frac{\partial a_2}{\partial T} = f_2^- a_2 + db_2^* + [DA_0(2a_1 b_1^* + a_1^2)] + a_1 \delta + a_3 \delta^*, \quad (2.7)$$

$$\frac{\partial b_2}{\partial T} = da_2^* + f_2^+ b_2 + [DA_0(2a_1^* b_1 + b_1^2)] + b_1 \delta^* + b_3 \delta \dots \quad (2.8)$$

where $f_0 = \Delta_0 - \beta q^2 - i\gamma$, $f_n^\pm = \Delta_0 - \beta(q \pm nk)^2 - i\gamma + 2DA_0^2$, $d = DA_0^2$, and the Y -dependence of the values A_0 , a_n , b_n has been neglected for the sake of simplicity.

The nonlinear dynamics in the system (2.4-2.8) depend on the forcing parameters and the convection intensity, with the modulation wave-vector k being the key factor for pattern formation. Below we briefly describe several limiting cases.

In the linear approximation in $|\delta/\Delta_0| \ll 1$, the solution (2.2) satisfies equation (2.4), while the equations (2.5,2.6) are reduced to:

$$\frac{\partial a_1}{\partial T} = f_1^- a_1 + db_1^* + A_0 \delta, \quad \frac{\partial b_1}{\partial T} = da_1^* + f_1^+ b_1 + A_0 \delta. \quad (2.9)$$

The linear system (2.9) has steady solutions with

$$a_1 = A_1 = -\frac{A_0\delta\left((f_1^+)^* - d\right)}{\left(f_1^- (f_1^+)^* - dd^*\right)}, \quad b_1^* = B_0^* = -\frac{A_0\delta\left(f_1^- - d^*\right)}{\left(f_1^- (f_1^+)^* - dd^*\right)}. \quad (2.10)$$

The solutions (2.2,2.3,2.10) are stable for $Re[\sigma] < 0$, where the Liapunov exponents σ obey the equation

$$(\sigma + 2f_0) \left[(\sigma - f_1^-) \left(\sigma - (f_1^+)^* \right) - dd^* \right] = 0. \quad (2.11)$$

For the large-scale modulations with $k/q \ll 1$, pattern formation is quite complicated. In the interval $\beta_r q^2 < \Delta_0 < F_r$, the pure solution with A_0 from (2.2) and $a_1 = b_1 = 0$ occurs, where $F_r = F_r(D, \beta)$ and $F_r > \beta_r$. For $\Delta_0 > F_r q^2$, this solution becomes unstable, and the modulated pattern (2.3,2.10) appears. In the limit of $(k/q) \rightarrow 0$, the values of $|a_1|, |b_1|$ increase as $|\delta/\Delta_0|(q/k)^2$, and result in a growth of the higher-order terms in the system (2.5-2.8). A nonlinear coupling among the amplitudes a_n and b_n yields then a solution with $|a_n/A_0|, |b_n/A_0| \gg |\delta/\Delta_0|$, yet keeping $|a_n/A_0| \ll 1$. In this case the system (2.5-2.8) is reduced to

$$\frac{\partial a_1}{\partial T} = f_1^- a_1 + db_1^* + [D(a_1 a_1^* + 2b_1 b_1^*) a_1 + 2DA_0(a_1^* a_2 + a_2 b_1 + b_1 b_2^*)], \quad (2.12)$$

$$\frac{\partial b_1}{\partial T} = da_1^* + f_1^+ b_1 + [D(2a_1 a_1^* + b_1 b_1^*) b_1 + 2DA_0(a_1 a_2^* + a_1 b_2 + b_1^* b_2)], \quad (2.13)$$

$$\frac{\partial a_2}{\partial T} = f_2^- a_2 + db_2^* + [DA_0(2a_1 b_1^* + a_1^2)], \quad (2.14)$$

$$\frac{\partial b_2}{\partial T} = da_2^* + f_2^+ b_2 + [DA_0(2a_1^* b_1 + b_1^2)]. \quad (2.15)$$

From (2.12-2.15) we obtain

$$a_n = A_n e^{inGT}, \quad b_n = B_n e^{inGT}, \quad n = 1, 2, 3, \quad (2.16)$$

with A_2, B_2 dependent on $A_1 = A_1(\Delta_0, k, q)$ and $B_1 = B_1(\Delta_0, k, q)$. Using the solvability conditions for real A_1, B_1 , in (2.12-2.15), we derive the dispersion relation $G = G(\Delta_0, k, q)$. It is remarkable that $G \sim \gamma$ for small q and for $(k/q) \ll 1$. The solutions and their stability analysis are quite cumbersome and not presented here.

For the small-scale forcing with $k/q \gg 1$, the modulated state (2.3,2.10) is stable for all $\Delta_0 > 0$. The nonlinear dynamics in this case are governed by terms proportional to δ in (2.5-2.8), and the nonlinear solutions are steady. With $a_2 = b_2 = 0$, equations (2.4,2.5) are reduced to

$$\frac{\partial a_1}{\partial T} = A_0\delta + D(a_1 a_1^* + 2b_1 b_1^*) a_1, \quad (2.17)$$

$$\frac{\partial b_1}{\partial T} = A_0 \delta^* + D(2a_1 a_1^* + b_1 b_1^*) b_1, \quad (2.18)$$

and for small but finite $|\delta/\Delta_0|$ in the system (2.17,2.18)

$$a_1, b_1 \sim A_0 |\delta/\Delta_0|^{2/3}. \quad (2.19)$$

We conclude that the large-scale forcing eventually results in the occurrence of Rossby waves with quasi-periodic time-dependence. The convective pattern (2.3,2.16) consists of three traveling waves with different group velocities. The dynamics of this pattern depends on the convection intensity and the forcing wave-vector, yet it is independent of the forcing amplitude. In contrast, the small-scale forcing produces spatially modulated convective patterns with dynamics governed by the forcing amplitude.

3. Numerical results

To obtain numerical solutions of the complex amplitude A in (2.1), we non-dimensionalize this equation first using the length of the domain L , the reference time scale Δ_0^{-1} , and the initial magnitude of A_0 . This leads to the following equation:

$$\frac{\partial A'}{\partial T'} = \beta' \frac{\partial^2 A'}{\partial Y'^2} + A' + D' |A'|^2 A' + \tilde{\delta}' A' \quad (3.1)$$

The initial solution of the problem has the form $A = A_0 e^{iqY}$, and the forcing is defined as $\tilde{\delta} = \delta e^{ikY} + \delta^* e^{-ikY}$. The non-dimensional quantities are given by $A' = A/A_0$, $Y' = Y/L$, $T' = T\Delta_0$, $\beta' = \beta/\Delta_0 L^2$, $D' = D A_0^2/\Delta_0$ and $\tilde{\delta}' = \tilde{\delta}/\Delta_0$, and with the wavenumbers k and q being $k' = kL$ and $q' = qL$.

We solve equation (3.1) on a domain of length $L = 10$ with periodic boundary conditions. We replace the complex equation by a set of two equations for the real and imaginary parts of A . This set of equations is discretized using a second order central difference scheme in space. A fully implicit solver is used in time.

For these computations we choose $\Delta_0 = 100$ and $A_0 = 1$. The values of β and D are taken to match experiments of Herrmann & Busse (1998); Westerburg & Busse (2001). The three remaining parameters are the forcing amplitude δ and the ratio between the two wavenumbers k and q . Several cases have been computed with $\delta/\Delta_0 = 0.1, 0.2, 0.4, 0.6, 0.8, 1$, and $(k/q) = 1/10, 1/3, 1, 3, 10$. The space is discretized with a 300 points mesh, and the time step is chosen to be $\Delta T = 0.05$.

Figure 1 presents the real part of A' in (3.1) for the case with no forcing. The pattern has the form of the traveling wave, and its dynamics agrees qualitatively and quantitatively with the solution (2.2).

Figures 2, 3, and 4 show the real part of the amplitude, and the spatial and temporal Fourier transforms in the case of large-scale forcing with $k/q = 1/3$ and $\delta/\Delta_0 = 0.2$. Three traveling waves with different group velocities, described in (2.19), are clearly visible on the Figure 2. The spatio-temporal characteristics of the pattern are in good agreement with the results in (2.16). Figure 3 shows that the asymptotic dynamics of

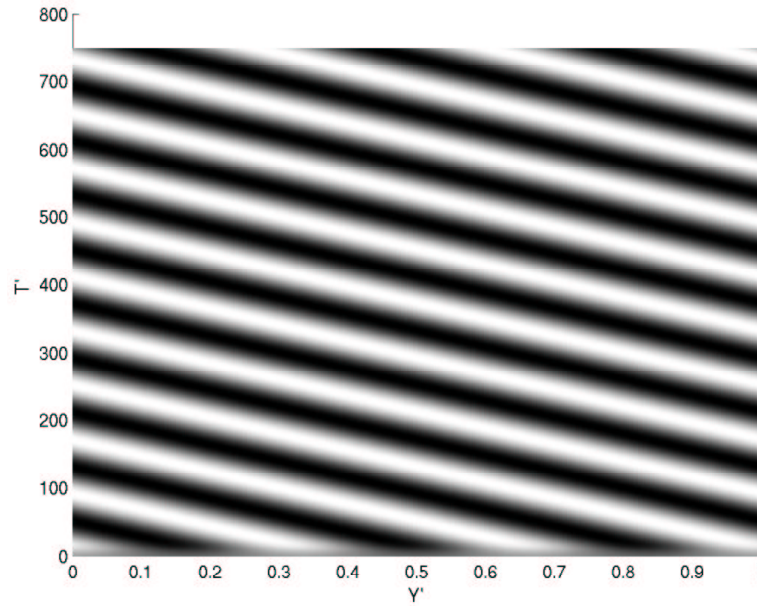


FIGURE 1. Rossby waves with no forcing

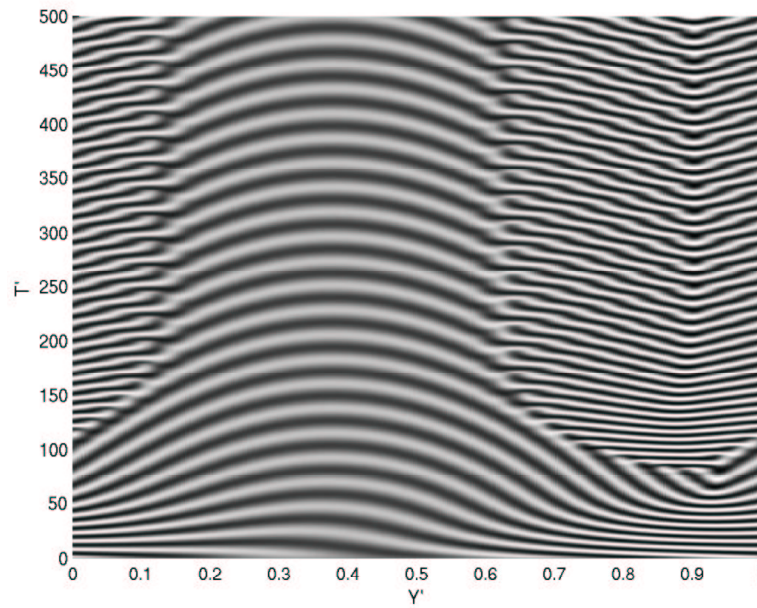


FIGURE 2. Real part of the amplitude in the case of large-scale modulation

the pattern are highly nonlinear, and there exist three major spatial modes associated with the wavevectors q , $q - k$ and $q + k$. Temporal Fourier transforms of the pattern on presented Figure 4 clearly show the existence of a low frequency, associated with small $(\gamma - G) \ll \gamma$ in (2.16). The other modes on Figure 4 correspond to γ in the equation (2.2) and $(\gamma + G) \sim 2\gamma$ in the solution (2.16). We conclude that the large-scale forcing

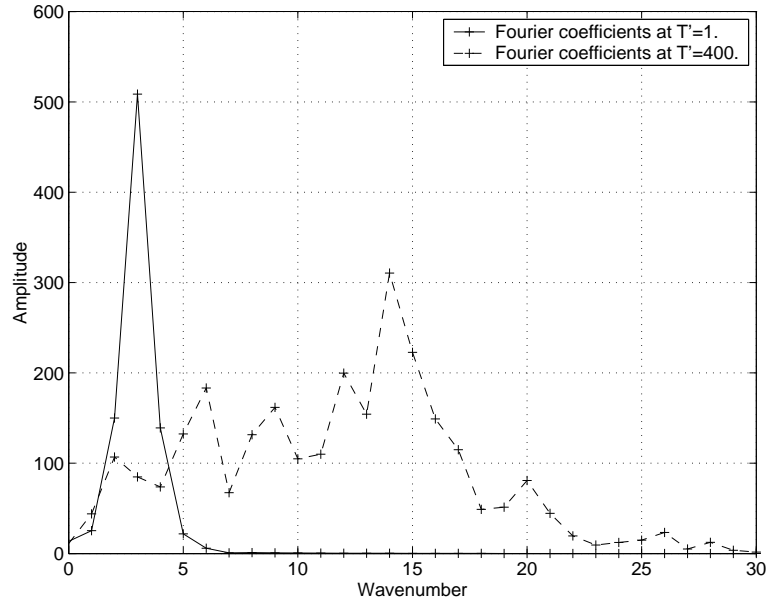


FIGURE 3. Spatial Fourier transform of the amplitude in the case of large-scale modulation

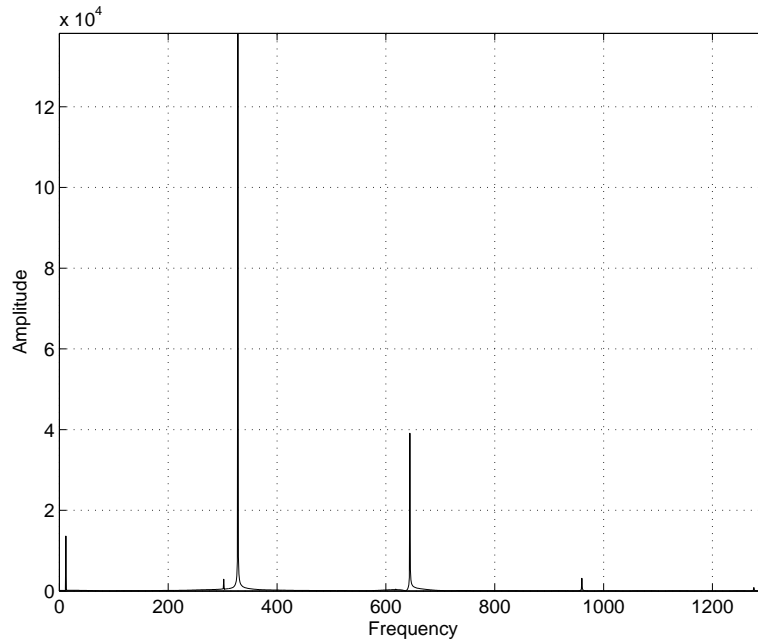


FIGURE 4. Temporal Fourier transform of the amplitude in the case of large-scale modulation

influences the Rossby waves significantly, and forms a pattern modulated in space and quasi-periodically in time.

Figures 5, 6, and 7 present the real part of the amplitude, and the spatial and temporal Fourier transforms in the case of small-scale forcing with $k/q = 10$ and $\delta/\Delta_0 = 0.1$. The pattern formation in this case differs significantly from that of the large-scale modula-

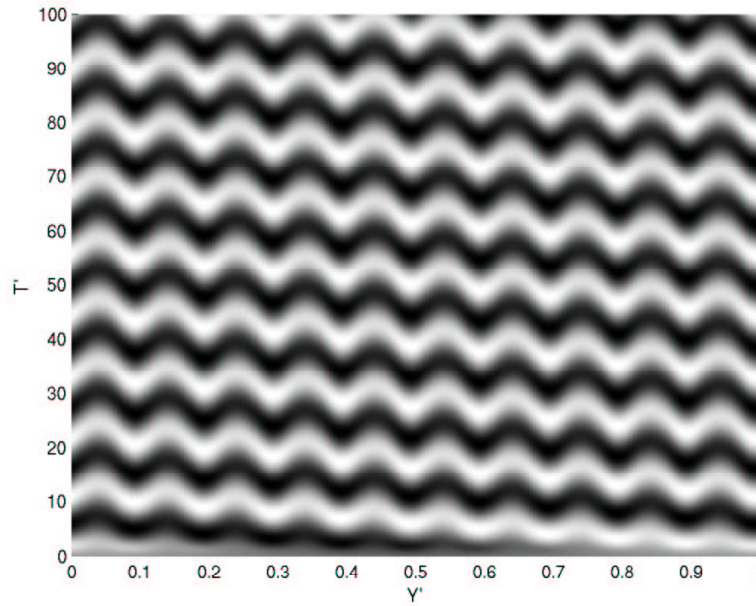


FIGURE 5. Real part of the amplitude in the case of small-scale modulation

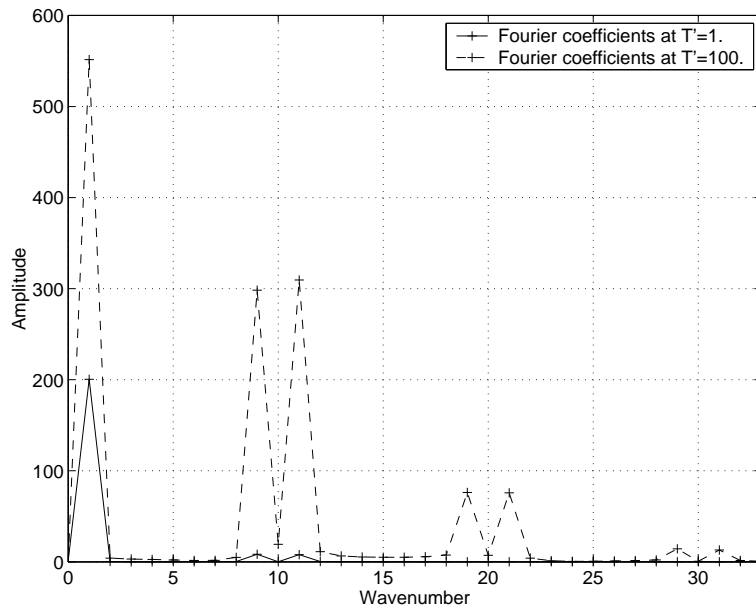


FIGURE 6. Spatial Fourier transform of the amplitude in the case of small-scale modulation

tions. Figures 5, 6, and 7 clearly show the formation of spatially modulated Rossby waves, in agreement with the solution (2.19). Figure 6 demonstrates that the spatial dynamics of the pattern are described by the modes associated with the wavevectors q , $q - k$ and $q + k$. Temporal Fourier transforms of the pattern shown on Figure 7 indicate that there

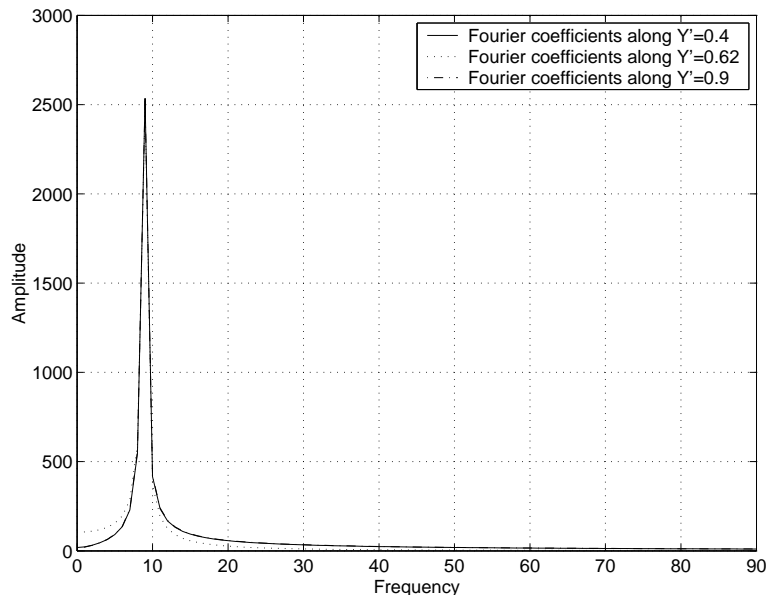


FIGURE 7. Temporal Fourier transform of the amplitude in the case of small-scale modulation

is only one frequency in the system, which is associated with γ in (2.2). We conclude that the small-scale forcing modulates Rossby waves in space, (2.19).

4. Discussion

In the present work, we studied the effect of surface topography on the nonlinear dynamics of thermal Rossby waves. The foregoing results show that the interaction of Rossby waves with spatially modulated forcing gives rise to a quasi-periodic behavior in space as well in time. The large-scale forcing results in the appearance of interacting traveling waves, whose dynamics depend strongly on the forcing wavevector and weakly on the convection intensity, and are insensitive to the forcing amplitude. In contrast, the small-scale forcing generates spatially modulated patterns, but does not influence their temporal dependence. In this case, the pattern dynamics are governed by the forcing amplitude and the convection intensity.

Our model captures the main properties of the linear and weakly nonlinear solutions obtained in Bell & Soward (1996) and Westerburg & Busse (2001). On the other hand, the model describes the influence of modulations on the dynamics of Rossby waves in a wide range of the forcing parameters and convection intensity, and predicts the new properties of the nonlinear dynamics. Our results are in a good qualitative agreement with the observations by Westerburg & Busse (2001).

REFERENCES

- ALDRIDGE, K., BLOXHAM, J., DEHANT, V. *et al.* 1990 Core-Mantle interactions. *Surv. Geophys.* **11**, 329–353.
- ARANSON, I. & KRAMER, L. 2002 The world of the complex Ginzburg-Landau equation. *Rev. Mod. Phys.* **74**, 99–143.

- BELL, P. & SOWARD, A. 1996 The influence of surface topography on rotating convection. *J. Fluid Mech.* **313**, 147–180.
- BUSSE, F. & OR, A. 1986 Convection in a rotating cylindrical annulus - thermal Rossby waves. *J. Fluid Mech.* **166**, 173–187.
- COULLET, P., LEGA, J., HOCHMANZADEH, B. *et al.* 1990 Breaking chirality in nonequilibrium systems. *Phys. Rev. Lett.* **65**, 1352–1355.
- CROSS, M. & HOHENBERG, P. 1993 Pattern formation outside of equilibrium. *Rev. Mod. Phys.* **65**, 851–1112.
- ELPHICK, C., IOOSS, G. & TIRAPEGUI, E. 1987 Normal-form reduction of time-periodically driven differential equations. *Phys. Lett. A* **120**, 459–463.
- HEMMING, C. & KAPRAL, R. 2000 Resonantly forced inhomogeneous reaction-diffusion systems. *Chaos* **10**, 720–730.
- HERRMANN, J. & BUSSE, F. 1998 Stationary and time dependent convection in the rotating cylindrical annulus with modulated height. *Phys. Phys. Fluids* **10**, 1611–1620.
- HIDE, R. 1971 Geostrophic motion of a non-homogeneous fluid. *J. Fluid Mech.* **49**, 745.
- KUANG, W. & BLOXHAM, J. 1999 Numerical modeling of magnetohydrodynamic convection in a rapidly rotating spherical shell: Weak and strong field dynamo action. *J. Comp. Phys.* **153**, 51–81.
- MATTHEWS, P. & COX, S. 2000 Pattern formation with a conservation law. *Nonlinearity* **13**, 1293–1320.
- MEYER, C., AHLERS, G. & CANNELL, D. 1987 Initial stages of pattern formation in Rayleigh-Benard convection. *Phys. Rev. Lett.* **59**, 1577–1580.
- OR, A. & BUSSE, F. 1987 Convection in a rotating cylindrical annulus. 2. Transitions to asymmetric and vacillating flow. *J. Fluid Mech.* **174**, 313–326.
- RODER, J., RODER, H. & KRAMER, L. 1997 Linear stability analysis of bifurcations with a spatially periodic, fluctuating control parameter. *Phys. Rev. E* **55**, 7068–7078.
- SIGGIA, E. & ZIPPELIUS, A. 1981 Pattern selection in Rayleigh-Benard convection near threshold. *Phys. Rev. Lett.* **47**, 835–838.
- TRIBELSKY, M.I. & VELARDE, M.G. 1996 Short-wavelength instability in systems with slow long-wavelength dynamics. *Phys. Rev. E* **54**, 4973–4981.
- WESTERBURG, M. & BUSSE, F. 2001 Finite-amplitude convection in the presence of finitely conducting boundaries. *J. Fluid Mech.* **432**, 351–367.
- WU, M. & ANDERHECK, C. 1990 Effect of external noise on the Fredericksz transition in a nematic liquid crystal. *Phys. Rev. Lett.* **65**, 591–594.
- ZHANG, K., EARNSHAW, P., LIAO, X. *et al.* 2001 On inertial waves in a rotating fluid sphere. *J. Fluid Mech.* **437**, 103–119.